

Article

Optimization Production of an Endo- β -1,4-Xylanase from *Streptomyces thermocarboxydus* Using Wheat Bran as Sole Carbon Source

Thi Ngoc Tran ¹, Chien Thang Doan ¹, Thi Kieu Loan Dinh ², Thi Hai Ninh Duong ¹,
Thi Thuc Uyen Phan ¹, Thi Thuy Loan Le ¹, Trung Dung Tran ¹, Pham Hung Quang Hoang ¹,
Anh Dzung Nguyen ³ and San-Lang Wang ^{4,5,*}

¹ Faculty of Natural Science and Technology, Tay Nguyen University, Buon Ma Thuot 630000, Vietnam; ttingoc@ttn.edu.vn (T.N.T.); dcthang@ttn.edu.vn (C.T.D.); dthninh@ttn.edu.vn (T.H.N.D.); pttuyen@ttn.edu.vn (T.T.U.P.); lttloan@ttn.edu.vn (T.T.L.L.); ttdung@ttn.edu.vn (T.D.T.); hphquang@ttn.edu.vn (P.H.Q.H.)

² Faculty of Education, Tay Nguyen University, Buon Ma Thuot 630000, Vietnam; dtkloan@ttn.edu.vn

³ Institute of Biotechnology and Environment, Tay Nguyen University, Buon Ma Thuot 630000, Vietnam; nadzung@ttn.edu.vn

⁴ Department of Chemistry, Tamkang University, New Taipei City 25137, Taiwan

⁵ Life Science Development Center, Tamkang University, New Taipei City 25137, Taiwan

* Correspondence: sabulo@mail.tku.edu.tw

Abstract: Xylanases, key enzymes for hydrolyzing xylan, have diverse industrial applications. The bioprocessing of agricultural byproducts to produce xylanase through fermentation approaches is gaining importance due to its significant potential to reduce enzyme production costs. In this work, the productivity of *Streptomyces thermocarboxydus* TKU045 xylanase was enhanced through liquid fermentation employing wheat bran as the sole carbon source. The maximum xylanase activity (25.314 ± 1.635 U/mL) was obtained using the following optima factors: 2% (*w/v*) wheat bran, 1.4% (*w/v*) KNO_3 , an initial pH of 9.8, an incubation temperature of 37.3 °C, and an incubation time of 2.2 days. Xylanase (Xyn_TKU045) of 43 kDa molecular weight was isolated from the culture supernatant and was biochemically characterized. Analysis through liquid chromatography with tandem mass spectrometry revealed a maximum amino acid identity of 19% with an endo-1,4- β -xylanase produced by *Streptomyces lividans*. Xyn_TKU045 exhibited optimal activity at pH 6, with remarkable stability within the pH range of 6.0 to 8.0. The enzyme demonstrated maximum efficiency at 60 °C and considerable stability at ≤ 70 °C. Mg^{2+} , Mn^{2+} , Ba^{2+} , Ca^{2+} , 2-mercaptoethanol, Tween 20, Tween 40, and Triton X-100 positively influenced Xyn_TKU045, while Zn^{2+} , Fe^{2+} , Fe^{3+} , Cu^{2+} , and sodium dodecyl sulfate exhibited adverse impact. The kinetic properties of Xyn_TKU045 were a K_m of 0.628 mg/mL, a k_{cat} of 75.075 s^{-1} and a k_{cat}/K_m of $119.617 \text{ mL mg}^{-1}\text{s}^{-1}$. Finally, Xyn_TKU045 could effectively catalyze birchwood xylan into xylotriose and xylobiose as the major products.

Keywords: agricultural residue; optimization production; *Streptomyces thermocarboxydus*; wheat bran; xylanase



Citation: Tran, T.N.; Doan, C.T.; Dinh, T.K.L.; Duong, T.H.N.; Phan, T.T.U.; Le, T.T.L.; Tran, T.D.; Hoang, P.H.Q.; Nguyen, A.D.; Wang, S.-L. Optimization Production of an Endo- β -1,4-Xylanase from *Streptomyces thermocarboxydus* Using Wheat Bran as Sole Carbon Source. *Recycling* **2024**, *9*, 50. <https://doi.org/10.3390/recycling9030050>

Academic Editor: Salustiano Mato De La Iglesia

Received: 31 March 2024

Revised: 5 June 2024

Accepted: 5 June 2024

Published: 9 June 2024



Copyright: © 2024 by the authors. Licensee MDPI, Basel, Switzerland. This article is an open access article distributed under the terms and conditions of the Creative Commons Attribution (CC BY) license (<https://creativecommons.org/licenses/by/4.0/>).

1. Introduction

Xylanases, classified as endo-1,4- β -d-xylanohydrolase (EC 3.2.1.8), are hemicellulases commonly employed in processes such as pulp bleaching and paper deinking [1]. Furthermore, these enzymes exhibit remarkable versatility and can be used in diverse sectors such as alternative fuel generation, baking, prebiotic preparation, and the clarification of fruit juices [2–6]. The source of this enzyme has primarily been associated with various fungi (for example, *Fusarium* [2], *Trichoderma* [7], *Aspergillus* [8], *Thielavia* [9], and *Rhizomucor* [10]), and bacteria (for example, *Bacillus* [4], *Streptomyces* [11], *Paenibacillus* [12], and *Halomonas* [13]), showcasing the diverse microbial sources of this enzyme. Among

the strains, *Streptomyces*, a bacterial genus renowned for its prolific production of various enzymes, including xylanases, holds promise for industrial applications. The unique characteristics of *Streptomyces* make it an interesting subject for further research and development in the section of enzymology and biotechnology. This species was reported for its capacity to generate thermostable xylanases that remain active at elevated temperatures (≥ 60 °C) [14,15]. *Streptomyces* strains also exhibit the capability to utilize a diverse array of carbon and nitrogen sources, including various types of residues, for the biosynthesis of enzymes [16–20], including xylanase [21–23].

The utilization of xylan as the source of carbon and an inducer for xylanase production poses certain economic challenges due to its high cost of production. To address this issue, researchers have explored substituting commercially available xylan with low-cost and readily available agricultural by-products, resulting in a significant reduction in the cost of overall processing [24]. This innovative approach, utilizing abundant agricultural residues, opens avenues for the cost-effective production of xylanase. By tapping into these agricultural residues, the production costs can be minimized and the sustainable utilization of waste materials can be promoted, aligning with eco-friendly practices in enzyme production. A vast array of agricultural residues, such as sugarcane bagasse [25], rice straw [26], rice bran [27], wheat bran [28], coconut husk [29], corn stalk [30], and corncob [31], can be used as the carbon source or both carbon and nitrogen sources for microbial xylanase synthesis.

Maximizing productivity yield is an essential step for the industrial applications of enzymes. Culture conditions can be optimized using the one-factor-at-a-time (OFAT) method. However, this approach does not account for interactions between factors. To address this limitation, response surface methodology (RSM) has been effectively used as an alternative in optimization solutions. Indeed, RSM has been effectively applied to maximize xylanase productivity [26]. In a previous study, a potential xylanase-producing strain, *Streptomyces thermocarboxydus* TKU045 demonstrated the ability to utilize wheat bran powder (WBP) as the exclusive carbon source and exhibited elevated xylanase activity [32]. However, the enzyme production was not statistically optimized, and the purification process was not performed at that time. Therefore, our objective was to figure out the cultivation conditions for maximizing xylanase productivity using RSM combined with Box–Behnken design (BBD), followed by its purification for subsequent biochemical characterization.

2. Results and Discussion

2.1. Production Optimization of *Streptomyces thermocarboxydus* TKU045 Xylanase Using Wheat Bran Powder as the Sole Carbon Source

Optimizing medium and culture parameters is crucial for a significant improvement in xylanase productivity, a goal achievable through response surface methodology (RSM) [3,4,33]. This approach comprehensively examines the interactive impacts of all independent factors in a fermentation process and investigates the specific interactions between a response variable and a series of design-independent variables [3], which the OFAT method cannot achieve. The Box–Behnken design (BBD), a top-rated design of RSM [34], was employed to optimize the xylanase productivity of *S. thermocarboxydus* TKU045, incorporating five factors: the amount of WBP (X_1), the amount of KNO_3 (X_2), initial pH (X_3), incubation temperature (X_4), and incubation time (X_5). The BBD comprises of 46 runs; the highest xylanolytic activity (26.978 U/mL) was noted at run 42 (Table 1). The data were subjected to regression fitting to derive the regression formula for the second-order model:

$$Y \text{ (xylanase activity, U/mL)} = -2167.2 + 39.162X_1 + 138.53X_2 + 180.64X_3 + 61.012X_4 + 34.787X_5 - 11.173X_1 \times X_1 - 27.745X_2 \times X_2 - 9.016X_3 \times X_3 - 0.781X_4 \times X_4 - 10.187X_5 \times X_5 - 0.375X_1 \times X_2 + 0.431X_1 \times X_3 - 0.042X_1 \times X_4 + 1.680X_1 \times X_5 - 1.115X_2 \times X_3 - 1.261X_2 \times X_4 - 1.678X_2 \times X_5 - 0.131X_3 \times X_4 + 0.548X_3 \times X_5 + 0.122X_4 \times X_5$$

Table 1. The results of the Box–Behnken design experiment.

Run	Coded Levels					Uncoded Levels					Y (U/mL)
	X ₁	X ₂	X ₃	X ₄	X ₅	X ₁	X ₂	X ₃	X ₄	X ₅	
1	−1	−1	0	0	0	1	1	10	37	2	8.494
2	+1	−1	0	0	0	3	1	10	37	2	9.396
3	−1	+1	0	0	0	1	2	10	37	2	1.500
4	+1	+1	0	0	0	3	2	10	37	2	1.651
5	0	0	−1	−1	0	2	1.5	9	34	2	14.488
6	0	0	+1	−1	0	2	1.5	11	34	2	0.043
7	0	0	−1	+1	0	2	1.5	9	40	2	16.373
8	0	0	+1	+1	0	2	1.5	11	40	2	0.355
9	0	−1	0	0	−1	2	1	10	37	1	2.613
10	0	+1	0	0	−1	2	2	10	37	1	0.561
11	0	−1	0	0	+1	2	1	10	37	3	14.571
12	0	+1	0	0	+1	2	2	10	37	3	9.163
13	−1	0	−1	0	0	1	1.5	9	37	2	6.858
14	+1	0	−1	0	0	3	1.5	9	37	2	5.093
15	−1	0	+1	0	0	1	1.5	11	37	2	0.086
16	+1	0	+1	0	0	3	1.5	11	37	2	0.045
17	0	0	0	−1	−1	2	1.5	10	34	1	0.365
18	0	0	0	+1	−1	2	1.5	10	40	1	0.624
19	0	0	0	−1	+1	2	1.5	10	34	3	10.960
20	0	0	0	+1	+1	2	1.5	10	40	3	12.687
21	0	−1	−1	0	0	2	1	9	37	2	18.841
22	0	+1	−1	0	0	2	2	9	37	2	12.625
23	0	−1	+1	0	0	2	1	11	37	2	8.638
24	0	+1	+1	0	0	2	2	11	37	2	0.193
25	−1	0	0	−1	0	1	1.5	10	34	2	8.998
26	+1	0	0	−1	0	3	1.5	10	34	2	6.257
27	−1	0	0	+1	0	1	1.5	10	40	2	9.622
28	+1	0	0	+1	0	3	1.5	10	40	2	6.374
29	0	0	−1	0	−1	2	1.5	9	37	1	2.645
30	0	0	+1	0	−1	2	1.5	11	37	1	0.000
31	0	0	−1	0	+1	2	1.5	9	37	3	11.229
32	0	0	+1	0	+1	2	1.5	11	37	3	10.778
33	−1	0	0	0	−1	1	1.5	10	37	1	0.526
34	+1	0	0	0	−1	3	1.5	10	37	1	0.680
35	−1	0	0	0	+1	1	1.5	10	37	3	4.983
36	+1	0	0	0	+1	3	1.5	10	37	3	11.855
37	0	−1	0	−1	0	2	1	10	34	2	12.385
38	0	+1	0	−1	0	2	2	10	34	2	8.163
39	0	−1	0	+1	0	2	1	10	40	2	18.121
40	0	+1	0	+1	0	2	2	10	40	2	6.335
41	0	0	0	0	0	2	1.5	10	37	2	26.148
42	0	0	0	0	0	2	1.5	10	37	2	26.978
43	0	0	0	0	0	2	1.5	10	37	2	22.187
44	0	0	0	0	0	2	1.5	10	37	2	22.402
45	0	0	0	0	0	2	1.5	10	37	2	26.188
46	0	0	0	0	0	2	1.5	10	37	2	23.790

X₁, amount of wheat bran powder (WBP; %); X₂, amount of KNO₃ (%); X₃, initial pH of medium; X₄, incubation temperature (°C); X₅, incubation time (day).

This regression equation was obtained using the result (mentioned in Table 2) generated by analyzing experimental data with the RSM function [35]. According to Table 2, the low *p*-value (*p* < 0.0001) and significant F-value (15.15) indicate that the model is significant. The high R² (0.9238) suggests that the model fits well with the data; only 7.62% of total variations could not be described by the model. In addition, the adjusted R² (0.8628) was also high, confirming the model’s significance. The analysis of variance based upon the *p*-value suggested that the linear terms (X₂, X₃, and X₄) and the quadratic terms (X₁²,

X_2^2 , X_3^2 , X_4^2 , and X_5^2) were significant. The lack of fit for the proposed model was not significant, indicating that it is fit for prediction, and hence the statistical implication of this theoretical account was turned over by the equations for coded factors (Table 3). As the two-factor interaction term was insignificant, the model was refined by removing this term from the regression formula to obtain the refined model, as follows:

$$Y = -2058.124 + 44.708X_1 + 76.627X_2 + 176.077X_3 + 57.970X_4 + 45.638X_4 - 11.173X_1^2 - 27.745X_2^2 - 9.016X_3^2 - 0.781X_4^2 - 10.187X_5^2$$

with an $R^2 = 0.9125$, an adjusted $R^2 = 0.8875$, an F-value = 36.5, and a p -value < 0.00001.

Table 2. Results of regression analysis using the Box–Behnken design.

Term	Coefficient Estimate	Standard Error Coefficient	t Value	Pr (> t)	
Constant	−2167.200	296.800	−7.302	<0.00001	***
X ₁	39.162	24.626	1.590	0.124	
X ₂	138.530	49.627	2.791	0.010	**
X ₃	180.640	28.006	6.450	<0.00001	***
X ₄	61.012	9.894	6.167	<0.00001	***
X ₅	34.787	24.626	1.413	0.170	
X ₁ X ₂	−0.375	2.983	−0.126	0.901	
X ₁ X ₃	0.431	1.491	0.289	0.775	
X ₁ X ₄	−0.042	0.497	−0.085	0.933	
X ₁ X ₅	1.680	1.491	1.126	0.271	
X ₂ X ₃	−1.115	2.983	−0.374	0.712	
X ₂ X ₄	−1.261	0.994	−1.268	0.216	
X ₂ X ₅	−1.678	2.983	−0.563	0.579	
X ₃ X ₄	−0.131	0.497	−0.264	0.794	
X ₃ X ₅	0.548	1.491	0.368	0.716	
X ₄ X ₅	0.122	0.497	0.246	0.808	
X ₁ ²	−11.173	1.010	−11.066	<0.00001	***
X ₂ ²	−27.745	4.038	−6.870	<0.00001	***
X ₃ ²	−9.016	1.010	−8.930	<0.00001	***
X ₄ ²	−0.781	0.112	−6.961	<0.00001	***
X ₅ ²	−10.187	1.010	−10.091	<0.00001	***

$R^2 = 0.9238$; Adjusted $R^2 = 0.8628$; F-statistic: 15.15 on 20 and 25 degrees of freedom (DF); p -value: 2.11×10^{-9} ; Significance codes: 0 '***' 0.001 '**' 0.01. X₁, amount of wheat bran powder (WBP; %); X₂, amount of KNO₃ (%); X₃, initial pH of medium; X₄, incubation temperature (°C); X₅, incubation time (day).

Table 3. The results of the analysis of variance for the fitted quadratic polynomial model.

Source	Degrees of Freedom	Sum of Squares	Mean Square	F Value	Pr (>F)
Fo	5	851.01	170.20	19.133	<0.00001
TWI	10	32.95	3.30	0.371	0.948
PQ	5	1811.54	362.31	40.729	<0.00001
Residuals	25	222.39	8.90		
Lack of fit	20	200.51	10.03	2.291	0.182
Pure error	5	21.88	4.38		

The interplay between two factors, with the others maintained at their midpoint (0) level, is represented in the two-dimensional (2D) contour plots (Figure S1) and 3D response surface plots (Figure S2). These plots exhibit peak xylanase activity near the midpoints (with 2% WBP, 1.5% KNO₃, pH 10, a temperature of 37 °C, and an incubation time of 2 days), indicating that the designated levels were within the suitable range. There was an interesting alignment between the plots and regression analysis, suggesting that the interaction among the factors was insignificant. Noticeably, increasing the values of the

factors led to a rise in xylanase productivity until the maximum value was achieved. However, a continued increase in these factors resulted in a corresponding decline in xylanase productivity. The optimal levels of WBP, pH, incubation temperature, and incubation time were estimated as 2%, 1.4%, 9.8, 37.3 °C, and 2.2 days, respectively, with a predicted xylanase productivity of 26.137 U/mL. Accordingly, a confirmation experiment was carried out by cultivating *S. thermocarboxydus* TKU045 under optimal conditions. The actual value of xylanase productivity was 25.314 ± 1.635 U/mL, which did not significantly differ from the predicted value (26.137 U/mL). There were relatively few reports on the statistical optimization of xylanase production from *Streptomyces* genus. By using the Central composite design of RSM, the optimal conditions for the xylanase production of *Streptomyces* sp. ER1 were 0.37% xylan and 33.10 mg/L olive oil [3]. The ideal conditions for the xylanase production of *Streptomyces variabilis* (MAB3), using the Box–Behnken design, were found to be 2% birchwood xylan, pH 8.2, a temperature of 46.5 °C, and an incubation time of 68 h [36]. Recently, Medouni-Haroune et al. (2024) reported the optimal conditions for the xylanase production of *Streptomyces* sp. S1M3I using the Box–Behnken design of RSM, which were 3% olive pomace powder, 0.3% (NH₄)₂SO₄, pH 7.4, and an incubation temperature of 40 °C [37]. It is evident that the optimal conditions for xylanase production vary. Therefore, determining the optimal enzyme production conditions for each strain of *Streptomyces* is an essential step. Furthermore, the optimization of xylanase produced by *S. thermocarboxydus* is rarely reported. Taken together, this study could be a novel observation of xylanase production optimization from the species *Streptomyces thermocarboxydus*.

2.2. Enzyme Purification

S. thermocarboxydus TKU045 was grown on a WBP-containing medium under optimized conditions. Subsequently, 1 L of the culture supernatant was harvested and precipitated with cold ethanol (−20 °C). While other studies commonly employ (NH₄)₂SO₄ to concentrate xylanase, our study reveals that xylanase activity through (NH₄)₂SO₄ precipitation was significantly low. In contrast, cold ethanol could retain nearly all xylanase activity (Table 4). Therefore, cold ethanol was employed as a substitute for (NH₄)₂SO₄. The crude enzyme was then loaded onto a High-Q column for initial purification. The chromatography profile for the separation of three xylanase activity peaks (F1, F2, and F3) with a NaCl gradient in the range of 0 to 0.5 M is shown in Figure 1a. This result aligned with our previous findings, in which the cultivation medium of *S. thermocarboxydus* TKU045 displayed multiple bands of xylanolytic activity on PAGE gel containing xylan [32]. All three peaks were desalted by dialysis and further purified using a DEAE sepharose column. However, only fraction F1 could be successfully purified, yielding a single protein band, as shown by SDS-PAGE (Figure 1b). In contrast, fractions F2 and F3 lost their activity completely during the subsequent purification step. Consequently, only one xylanase (Xyn_TKU045) was successfully purified.

Table 4. A summary of the purification of Xyn-TKU045.

Step	Total Protein (mg)	Total Activity (U)	Specific Activity (U/mg)	Recovery (%)	Purification (Fold)
Cultural supernatant	4858.7	26,111.0	5.4	100	1.0
Ethanol precipitation	2439.1	25,078.6	10.3	96	1.9
High Q column	57.7	10,857.8	188.1	42	35.0
DEAE sepharose column	3.2	3882.330	1212.7	15	225.7

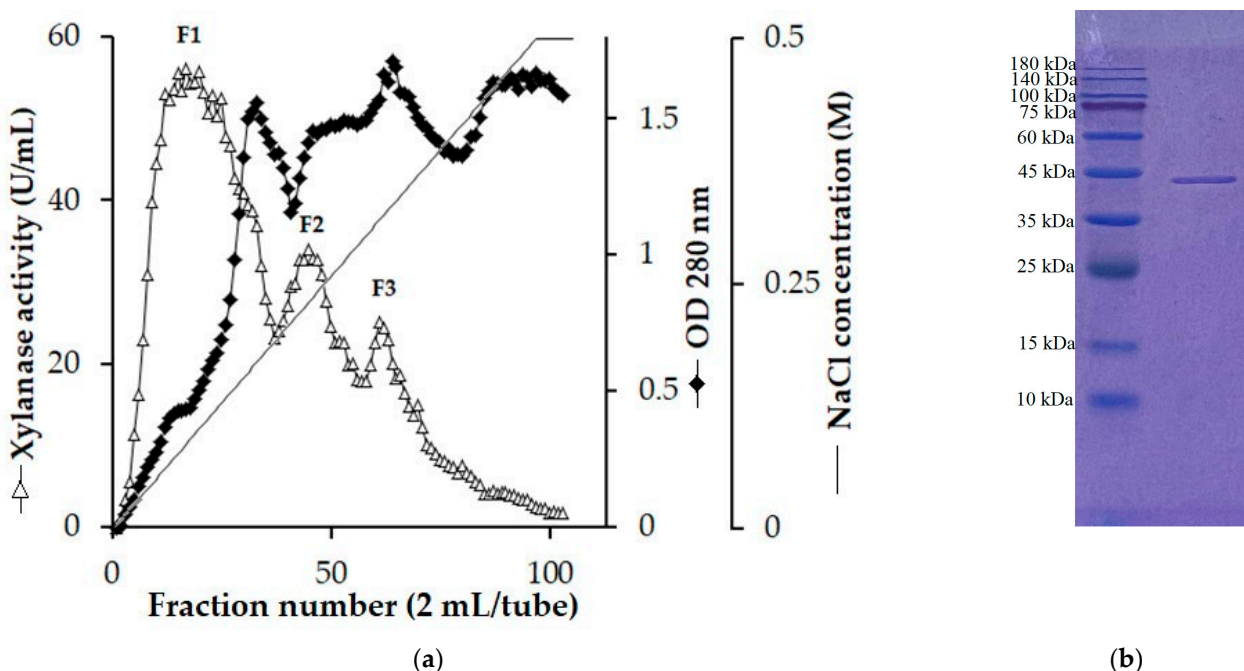


Figure 1. Chromatography profile of the crude enzyme on High-Q column (a), and sodium dodecyl sulfate-polyacrylamide gel electrophoresis profile of Xyn-TKU045 (b).

The molecular weight (MW) of Xyn_TKU045 was approximately 43 kDa (Figure 1b). This falls within the typical range of 15 kDa to 50 kDa for xylanases found in *Streptomyces* [32]. The MW of Xyn_TKU045 was comparable to that of *S. thermocarboxydus* HY-5’s xylanase (43.962 kDa) [38] and markedly inferior to that of *S. thermocarboxydus* MW8’s xylanase (52 kDa) [39].

To further verify the identity of the purified enzyme, the band corresponding to Xyn_TKU045 was excised from the SDS-PAGE gel, digested using trypsin, and subsequently analyzed using the LC-MS/MS method. The MASCOT search results, utilizing the Swissprot database and Firmicutes taxonomy, indicated the close association of xylanase with endo-1,4-beta-xylanase. The closest relative was identified as XYNA_STRLI (*Streptomyces lividans*) with 19% amino acid sequence identity (Table 5).

Table 5. Identification of Xyn_TKU045 using liquid chromatography with tandem mass spectrometry analysis.

Matched Peptide Sequence	Identified Protein and Coverage Rate	Strain
⁹⁰ IDATEPQR ⁹⁷	Endo-1,4-beta-xylanase 19%	<i>Streptomyces lividans</i>
¹⁴⁴ QAMIDHINGVMAHYK ¹⁵⁸		
¹⁶¹ IVQWDVVNEA FADGSSGAR ¹⁷⁹		
²⁰⁸ LCYNDYNVENWTWAK ²²²		
²⁴⁷ GVPIDCVGFQSHFNSGSPYNSNFR ²⁶⁰		
⁴¹⁸ VQIYSCWGGDNQK ⁴³⁰		

2.3. Biochemical Characterization

As illustrated in Figure 2a, the optimal pH of Xyn_TKU045 was determined to be pH 6 when assessed in a phosphate buffer. The enzyme exhibited remarkable activity, with over 80% maintained at both pH 7 and 8. This result suggests the versatility and effectiveness of the Xyn_TKU045 across a broad optimal pH spectrum from pH 6 to pH 8. Moreover, Xyn_TKU045 demonstrated robust stability within the pH range of 6 to 8. Studies published earlier have consistently found that the optimal pH for xylanases from

Streptomyces is typically from pH 5 to pH 7 [40–42]. The broad optimal pH range and stability observed in Xyn_TKU045 highlight its potential to function effectively under diverse pH conditions.

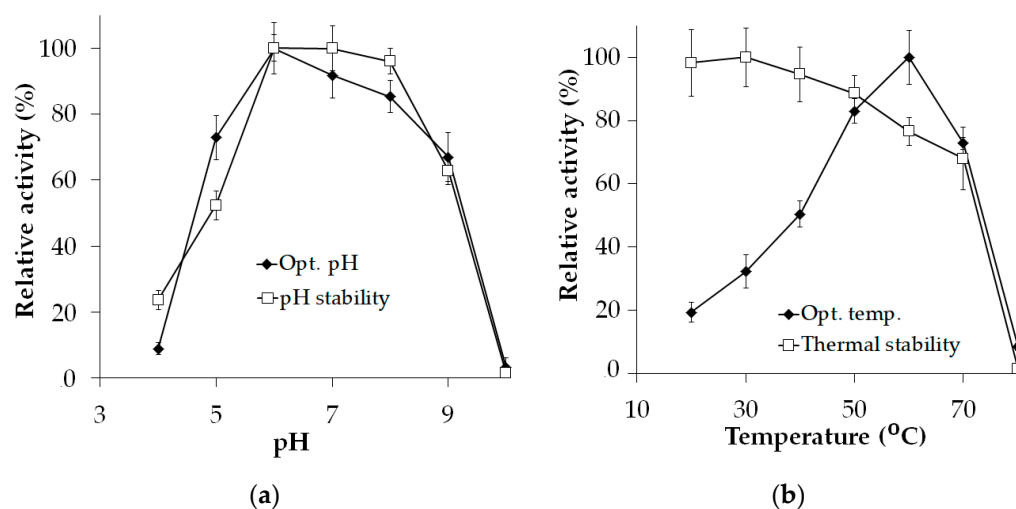


Figure 2. Effect of pH (a), and temperature (b) on the activity of xylanase Xyn_TKU045.

As illustrated in Figure 2b, the optimal temperature of Xyn_TKU045 was noted at 60 °C. When incubated at various temperature levels, Xyn_TKU045 maintained over 75% activity at temperatures up to 60 °C, while at 70 °C, the enzyme still retained approximately 68%. Thus, according to this study, Xyn_TKU045 is categorized as a thermophilic enzyme. Additionally, this xylanase displayed thermal stability (up to 60 °C) and activity (60 °C) comparable to or even better than most *Streptomyces* xylanases [21,40,43,44].

The impact of metal ions on Xyn_TKU045 was studied and the results are mentioned in Table 6. Metal ions that exhibited inhibitory effects include Zn^{2+} (2.676%), Fe^{2+} (51.140%), Fe^{3+} (0.793%), and Cu^{2+} (0.000%), whereas those that activate the enzyme comprise Mg^{2+} (142.616%), Mn^{2+} (219.029%), Ba^{2+} (168.682%), and Ca^{2+} (170.565%). Metal ions may exhibit variable effects among xylanases originating from different microbial strains. For instance, Ca^{2+} and Mn^{2+} exerted inhibitory effects on *Streptomyces matensis* DW67's xylanase [42], but they improved the activity of Xyn_TKU045 (this study) and *Streptomyces thermovulgaris* TISTR1948 [40]. Xyn_TKU045 was inactivated by Sodium lauryl sulfate (SDS), an anionic detergent with robust protein denaturing properties, highlighting the significance of hydrophobic interactions in preserving the 3D conformation of the protein. On the other hand, nonionic detergents (Tween 20, Tween 40, and Triton X-100) stimulated xylanase activity (164.420%, 161.943%, and 149.653%, respectively). The nonionic detergents enhance the disaggregation of proteins, thereby improving the hydrolysis activity of enzymes through the exposure of their catalytic sites. The exploration of the effect of 2-mercaptoethanol, a reducing agent, on enzyme activity revealed that it could simulate the activity of Xyn_TKU045 (166.501%) (Table 6). While 2-mercaptoethanol has already been recognized as a xylanase activity enhancer for certain *Streptomyces* strains [42,44], the xylanase derived from Xyn_TKU045 was unaffected by (Ethylenedinitrilo)tetraacetic acid (EDTA) (with a relative activity of $105.198 \pm 4.454\%$), indicating that it might not be a metalloenzyme.

Xyn_TKU045 demonstrated notable xylanolytic activity on three kinds of xylans (Table 7). However, Xyn_TKU045 could not hydrolyze non-xylan substrates such as starch, cellulose, and pectin. This substrate specificity emphasizes the tailored functionality of the enzyme, making it a promising candidate for applications that specifically target xylan-containing materials. Different amounts of birchwood xylan were used to determine the kinetic parameters for Xyn_TKU045. Accordingly, the K_m (reflects substrate affinity), k_{cat} (reflects catalytic rate), and k_{cat}/K_m (reflects catalytic efficiency) values for Xyn_TKU045 were 0.628 mg/mL, $75.075 s^{-1}$, and $119.617 mL mg^{-1}s^{-1}$, respectively. Li et al. (2022)

investigated the kinetic properties of xylanase derived from *Streptomyces* sp. T7 and found that the K_m and k_{cat}/K_m values for its activity on birchwood xylan were 2.78 mg/mL and 42.91 s⁻¹mg⁻¹, respectively [14]. In another report, the K_m , k_{cat} , and k_{cat}/K_m values for XynA from *S. rameus* L2001 were found to be 19.18 mg/mL, 1208.00 s⁻¹, 62.98 mL mg⁻¹s⁻¹, respectively [45].

Table 6. Effect of various chemicals on the activity of xylanase Xyn_TKU045.

Chemical	Relative Activity (%)
Control	100.000 ± 10.057
Zn ²⁺	2.676 ± 4.837
Fe ²⁺	51.140 ± 9.080
Fe ³⁺	0.793 ± 6.868
Cu ²⁺	0.000 ± 3.156
Mg ²⁺	142.616 ± 10.016
Mn ²⁺	219.029 ± 18.431
Ba ²⁺	168.682 ± 18.554
Ca ²⁺	170.565 ± 11.894
2-mercaptoethanol	166.501 ± 8.121
Tween 20	164.420 ± 5.252
Tween 40	161.943 ± 27.468
Triton X-100	149.653 ± 13.872
SDS	3.964 ± 5.152
EDTA	105.198 ± 4.454

Table 7. Substrate specificity of xylanase Xyn_TKU045.

Chemical	Relative Activity (%)
Birchwood xylan *	100.000 ± 6.585
Beechwood xylan	93.433 ± 6.935
Oatspelt xylan	95.646 ± 5.945
Starch	ND
Pectin	ND
Cellulose	ND

*, served as the control; ND, no xylanase activity detected.

2.4. Hydrolysis Pattern and Xylooligosaccharide Production

The xylan hydrolysis products after Xyn_TKU045 catalysis were analyzed using HPLC. As shown in Figure 3, after 30 min of hydrolysis, the obtained products were a mixture of xylooligosaccharides (XOSs). Upon extending the hydrolysis time, peaks corresponding to xylobiose (X₂) and xylobiose (X₃) were formed and became the predominant products. This outcome indicates that Xyn_TKU045 is an endo-enzyme. Additionally, starting from 2 h onwards, the HPLC analysis revealed a peak at the xylose position, suggesting that Xyn_TKU045 also exhibits exo-enzyme activity, albeit to a lesser extent. The presence of this xylose peak after 2 h implies that the exo-enzyme activity gradually manifested, providing insights into the enzyme's versatility in catalyzing both endo- and exo-type reactions during xylan hydrolysis. Numerous xylanases from *Streptomyces* have also been reported to primarily generate X₂ and X₃ during xylan hydrolysis [21,46–49].

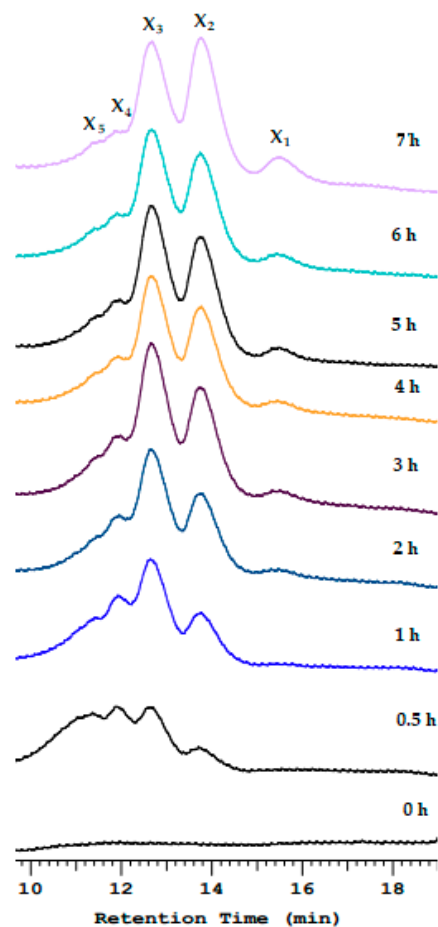


Figure 3. Hydrolysis pattern of *Streptomyces thermocarboxydus* TKU045 xylanase toward birchwood xylan. X₁, xylose; X₂, xylobiose; X₃, xylotriose; X₄, xylotetraose; X₅, xylopentose.

Low-molecular-weight XOSs, including X₂ and X₃, present significant commercial value as emerging prebiotics [50]. In a previous study, XOSs derived from xylan hydrolysis using *S. thermocarboxydus* TKU045's crude enzyme cocktail exhibited antioxidant and prebiotic activities on the *Bifidobacterium bifidum* BCRC 14615 [32]. Thus, it is interesting to explore the potential of Xyn_TKU045 as the biocatalyst for XOS production. To prepare XOSs, birchwood xylan (1%) was hydrolyzed by Xyn_TKU045 at different incubation times (from 0 h to 24 h). As illustrated in Figure S3, the concentration of reducing sugars reached its peak at 7.316 mg/mL after 6 h of incubation. Following this incubation period, the hydrolysate was subjected to HPLC analysis. The results indicated that 96% of hydrolysis products consisted of XOSs, while xylose accounted for only 4% of the total content. Interestingly, the analysis revealed that the majority of the XOSs were oligomers, with dimers and trimers making up 59% of the total XOSs present. Overall, the findings highlight that xylanase from *S. thermocarboxydus* TKU045 holds promise for producing bioactive low-molecular-weight XOSs.

3. Materials and Methods

3.1. Materials

The strain *Streptomyces thermocarboxydus* TKU045 was the same as was used in our previous work [32]. Xylose, xylan, and 3,5-dinitrosalicylic acid were obtained from Sigma Co. (St. Louis, MO, USA). Wheat bran was obtained from Miaoli (Miaoli City, Taiwan). Other chemicals were of the highest grade of purity.

3.2. Xylanase Assay and Protein Determination

The xylanase assay was conducted according to the method of Miller (1959) [51] using birchwood xylan [32]. Overall, the reaction component comprised 200 μL birchwood xylan (1%, pH 6, prepared sodium phosphate buffer) and 50 μL enzyme solution. This blend underwent incubation at 70 $^{\circ}\text{C}$ for 60 min, and 1500 μL DNS reagent was added and its concentration of reducing sugar was estimated through optical density (515 nm) measurement. An xylanase unit is determined by the enzyme quantity necessary to catalyze the liberation of 1 μmol product (equivalent to xylose) within one minute [32]. The protein was ascertained using the method of Lowry et al. (1951) [52].

3.3. Optimization of Production

The Box–Behnken design was employed for optimizing the response associated with five independent factors, namely, X_1 (the amount of WBP, % w/v), X_2 (the amount of KNO_3 , % w/v), X_3 (the initial pH of the medium), X_4 (incubation temperature, $^{\circ}\text{C}$), and X_5 (incubation time, days). The process was optimized using R-software (version 2021.09.1+372), with the “rsm” package employed for data analysis as well as graphical representation [35]. Forty-six runs, including 6 center points, were executed for optimization, and each factor was tested at three levels, low, medium, and high, represented, respectively, by the coded values of -1 , 0 , and $+1$. The determination of factor levels was guided by preliminary results obtained from experiments involving one-factor-at-a-time (OFAT) [32]. The resulting data were analyzed using R-software to establish the optimal conditions for xylanase production. The impact of the five examined factors was symbolized by the following quadratic formula:

$$Y = \beta_0 + \beta_1 X_1 + \beta_2 X_2 + \beta_3 X_3 + \beta_4 X_4 + \beta_5 X_5 + \beta_{12} X_1 \times X_2 + \beta_{13} X_1 \times X_3 + \beta_{14} X_1 \times X_4 + \beta_{15} X_1 \times X_5 + \beta_{23} X_2 \times X_3 + \beta_{24} X_2 \times X_4 + \beta_{25} X_2 \times X_5 + \beta_{34} X_3 \times X_4 + \beta_{35} X_3 \times X_5 + \beta_{45} X_4 \times X_5 + \beta_{11} X_1^2 + \beta_{22} X_2^2 + \beta_{33} X_3^2 + \beta_{44} X_4^2 + \beta_{55} X_5^2 \quad (1)$$

where Y is the predicted xylanase activity (U/mL); β_0 is the intercept; β_1 , β_2 , β_3 , β_4 , and β_5 are linear coefficients; β_{12} , β_{13} , β_{14} , β_{15} , β_{23} , β_{24} , β_{25} , β_{34} , β_{35} , and β_{45} are interactive coefficients; and β_{11} , β_{22} , β_{33} , β_{44} , and β_{55} are quadratic coefficients.

3.4. Enzyme Purification and Identification

For xylanase purification, the enzyme-containing culture supernatant was concentrated with cold ethanol at a ratio of 3:1 (ethanol/supernatant). The sediment was dissolved in Tris-HCl buffer (20 mM, pH 7.2) and then loaded onto a high Q column. A gradient elution of NaCl (0–1 M) was applied to isolate the xylanase. The xylanolytic fractions were dialyzed against Tris-HCl buffer and further purified using a DEAE column, followed by a Sephacryl S-200 column. The molecular weight and purity of the obtained protein were estimated using sodium dodecyl sulfate–polyacrylamide gel electrophoresis (SDS-PAGE) [53]. Liquid chromatography with tandem mass spectrometry (LC-MS/MS) analysis was performed to pinpoint the protein in the band on the SDS-PAGE gel [54].

3.5. Enzyme Characterization

The *S. thermocarboxydus* TKU045 xylanase’s optimal pH was assessed by measuring xylanolytic activity across a pH range of 4.0 to 10.0, using buffers such as acetate (pH 4.0 and 5.0), phosphate (pH 6.0, 7.0, and 8.0), and Tris-HCl (pH 9.0 and 10.0). To ascertain the ideal temperature, the xylanase assay conducted at varying temperatures from 20 to 80 $^{\circ}\text{C}$. To explore pH stability, the xylanase was kept at 20 $^{\circ}\text{C}$ for 60 min at various pH values (4.0–10.0) without substrate, and then residual activities were measured at pH 6.0. For assessing thermostability, the leftover activity was determined following individual incubations of *S. thermocarboxydus* TKU045 xylanase at temperatures ranging from 20 to 80 $^{\circ}\text{C}$ for 1 h.

The impact of various chemicals, including Tween 40, Tween 20, Sodium lauryl sulfate (SDS), Triton X-100, (Ethylenedinitrilo)tetraacetic acid (EDTA), Zn^{2+} , Fe^{2+} , Fe^{3+} , Cu^{2+} , Mg^{2+} , Mn^{2+} , Ba^{2+} , Ca^{2+} , and 2-mercaptoethanol, on xylanolytic activity were explored. Each chemical was introduced singly into the enzyme at a final concentration of 1 mM for 1 h. Subsequently, the effects of the chemicals were evaluated by measuring enzyme activities at pH 6.0 and 70 °C. As control, an enzyme solution without the addition of any chemical was used.

Birchwood xylan, beechwood xylan, oat spelt xylan, cellulose, pectin, and starch were used as the substrates to investigate the substrate specificity of the xylanase.

Various concentrations of xylan (ranging from 0.25 to 3 mg/mL) were utilized to determine the rate of the hydrolysis reaction catalyzed by Xyn_TKU045. Subsequently, a Lineweaver-Burk plot (Figure S4) was employed to calculate the kinetic parameters for xylanase, including K_m , k_{cat} , and k_{cat}/K_m .

Birchwood xylan was used as the substrate to assess the mechanism of hydrolysis of *S. thermocarboxydus* TKU045 xylanase. The hydrolysis products were analyzed at various time intervals (0, 0.5, 1, 2, 3, 4, 5, 6, and 7 h) through high-performance liquid chromatography (HPLC; column: KS-802; solvent: H₂O; flow rate: 0.6 mL/min; sample volume: 20 µL; column temperature: 80 °C; refractive index detector). For comparison, a standard mixture containing xylose (X₁), xylobiose (X₂), xylotriose (X₃), xyloetraose (X₄), and xylopentose (X₅) was utilized.

4. Conclusions

This research successfully demonstrated that *S. thermocarboxydus* TKU045 is an efficient xylanase producer using wheat bran-containing medium that could achieve a maximal productivity of 25.314 ± 1.635 U/mL. The isolated xylanase (Xyn_TKU045), characterized by an MW of 43 kDa, was purified and subjected to biochemical analysis from the culture. Xyn_TKU045 displayed optimal activity at pH 6.0 and 60 °C. Identified as an endo- β -1,4-xylanase, Xyn_TKU045 effectively catalyzed xylan into xylotriose and xylobiose as primary products.

Supplementary Materials: The following supporting information can be downloaded at: <https://www.mdpi.com/article/10.3390/recycling9030050/s1>, Figure S1: Two-dimensional (2D) contour plots showing the effect of the amount of wheat bran powder (WBP) and KNO₃ (a), WBP and pH (b), WBP and temperature (c), and WBP and incubation time (d). 2D contour plots showing the effect of the amount of KNO₃ and pH (e), KNO₃ and temperature (f), and KNO₃ and incubation time (g). 2D contour plots showing the effect of the pH and temperature (h), pH and incubation time (i), and temperature and incubation time (k); Figure S2: Response surface plots showing the effect of the amount of wheat bran powder (WBP) and amount of KNO₃ (a), WBP and pH (b), WBP and temperature (c), and WBP and incubation time (d). Response surface plots showing the effect of the amount of KNO₃ and pH (e), and KNO₃ and temperature (f), KNO₃ and incubation time (g). Response surface plots showing the effect of pH and temperature (h), pH and incubation time (i), and temperature and incubation time (k); Figure S3: Time courses of reducing sugar production generated from the hydrolysis of xylan catalyzed by Xyn_TKU045; Figure S4: Lineweaver-Burk plots of Xyn_TKU045.

Author Contributions: Conceptualization and methodology, T.N.T., C.T.D. and S.-L.W.; software, validation, formal analysis, investigation, resources, and data curation, T.N.T., C.T.D., T.D.T., P.H.Q.H., A.D.N., T.K.L.D., T.H.N.D., T.T.U.P. and T.T.L.L.; writing—original draft preparation, T.N.T. and C.T.D.; writing—review and editing, T.N.T., C.T.D. and S.-L.W.; visualization S.-L.W., T.N.T. and C.T.D.; supervision, project administration, and funding acquisition, S.-L.W. and T.N.T. All authors have read and agreed to the published version of the manuscript.

Funding: This study was supported in part by a grant from the National Science and Technology Council, Taiwan (NSTC-112-2320-B-032-001), and by a grant from Tay Nguyen University, Vietnam (T2023-43CBTĐ).

Data Availability Statement: Data are contained within the article and Supplementary Materials.

Conflicts of Interest: The authors declare no conflicts of interest.

References

1. Cruz-Davila, J.; Vargas Perez, J.; Sosa del Castillo, D.; Diez, N. *Fusarium graminearum* as a producer of xylanases with low cellulases when grown on wheat bran. *Biotechnol. Rep.* **2022**, *35*, e00738.
2. Kumari, K.; Goyal, S.; Maan, S. Hyper xylanase production and potential of xylooligosaccharides formation from a novel *Bacillus australimaris* KS2. *Biocatal. Agric. Biotechnol.* **2023**, *54*, 102899. [[CrossRef](#)]
3. Rosmine, E.; Sainjan, N.C.; Silvester, R.; Alikkunju, A.; Varghese, S.A. Statistical optimisation of xylanase production by estuarine *Streptomyces* sp. and its application in clarification of fruit juice. *J. Gen. Eng. Biotechnol.* **2017**, *15*, 393–401. [[CrossRef](#)]
4. Güler, F.; Özçelik, F. Screening of xylanase producing *Bacillus* species and optimization of xylanase process parameters in submerged fermentation. *Biocatal. Agric. Biotechnol.* **2023**, *51*, 102801. [[CrossRef](#)]
5. Wang, F.; Xu, H.; Wang, M.; Yu, X.; Cui, Y.; Xu, L.; Ma, A.; Ding, Z.; Huo, S.; Zou, B.; et al. Application of immobilized enzymes in juice clarification. *Foods* **2023**, *12*, 4258. [[CrossRef](#)]
6. Dhaver, P.; Pletschke, B.; Sithole, B.; Govinden, R. Optimization of xylooligosaccharides production by native and recombinant xylanase hydrolysis of chicken feed substrates. *Int. J. Mol. Sci.* **2023**, *24*, 17110. [[CrossRef](#)]
7. Alananbeh, K.M.; Alkfoof, R.; Muhaidat, R.; Massadeh, M. Production of xylanase by *Trichoderma* species growing on olive mill pomace and barley bran in a packed-bed bioreactor. *J. Fungi* **2024**, *10*, 49. [[CrossRef](#)]
8. Ameen, F. Purification and characterization of xylanase produced by *Aspergillus fumigatus* isolated from the northern border region of Saudi Arabia. *Fermentation* **2023**, *9*, 595. [[CrossRef](#)]
9. López-López, A.; Santiago-Hernández, A.; Cayetano-Cruz, M.; García-Huante, Y.; Campos, J.E.; Bustos-Jaimes, I.; Marsch-Moreno, R.; Cano-Ramírez, C.; Benitez-Cardoza, C.G.; Hidalgo-Lara, M.E. TtCel7A: A native thermophilic bifunctional cellulose/xylanase exoglucanase from the thermophilic biomass-degrading fungus *Thielavia terrestris* Co3Bag1, and its application in enzymatic hydrolysis of agroindustrial derivatives. *J. Fungi* **2023**, *9*, 152. [[CrossRef](#)]
10. Hüttner, S.; Granchi, Z.; Nguyen, T.T.; Pelt, S.V.; Larsbrink, J.; Thanh, V.N.; Olsson, L. Genome sequence of *Rhizomucor pusillus* FCH 5.7, a thermophilic zygomycete involved in plant biomass degradation harbouring putative GH9 endoglucanases. *Biotechnol. Rep.* **2018**, *20*, e00279. [[CrossRef](#)]
11. Wu, Q.; Zhang, C.; Zhu, W.; Lu, H.; Li, X.; Yang, Y.; Xu, Y.; Li, W. Improved thermostability, acid tolerance as well as catalytic efficiency of *Streptomyces rameus* L2001 GH11 xylanase by N-terminal replacement. *Enzym. Microb. Technol.* **2023**, *162*, 110143. [[CrossRef](#)]
12. Valenzuela, S.V.; Díaz, P.; Javier Pastor, F.I. Recombinant expression of an alkali stable GH10 xylanase from *Paenibacillus barcinonensis*. *J. Agric. Food Chem.* **2010**, *58*, 4814–4818. [[CrossRef](#)]
13. Veerakumar, S.; Manian, R. Agarase, Amylase and xylanase from *Halomonas meridiana*: A study on optimization of coproduction for biomass saccharification. *Fermentation* **2022**, *8*, 479. [[CrossRef](#)]
14. Li, Y.; Zhang, X.; Lu, C.; Lu, P.; Yin, C.; Ye, Z.; Huang, Z. Identification and characterization of a novel endo- β -1,4-xylanase from *Streptomyces* sp. T7 and its application in xylo-oligosaccharide production. *Molecules* **2022**, *27*, 2516. [[CrossRef](#)]
15. Li, N.; Meng, K.; Wang, Y.; Shi, P.; Luo, H.; Bai, Y.; Yang, P.; Yao, B. Cloning, expression, and characterization of a new xylanase with broad temperature adaptability from *Streptomyces* sp. S9. *Appl. Microbiol. Biotechnol.* **2008**, *80*, 231–240. [[CrossRef](#)]
16. Tran, T.N.; Doan, C.T.; Nguyen, V.B.; Nguyen, A.D.; Wang, S.L. The isolation of chitinase from *Streptomyces thermocarboxydus* and its application in the preparation of chitin oligomers. *Res. Chem. Intermed.* **2019**, *45*, 727–742. [[CrossRef](#)]
17. Tran, T.N.; Doan, C.T.; Nguyen, M.T.; Nguyen, V.B.; Vo, T.P.K.; Nguyen, A.D.; Wang, S.L. An Exochitinase with N-acetyl- β -glucosaminidase-like activity from shrimp head conversion by *Streptomyces speibonae* and its application in hydrolyzing β -chitin powder to produce N-acetyl-D-glucosamine. *Polymers* **2019**, *11*, 1600. [[CrossRef](#)]
18. Govindaraji, P.K.; Vuppu, S. Characterisation of pectin and optimization of pectinase enzyme from novel *Streptomyces fumigatiscleroticus* VIT-SP4 for drug delivery and concrete crack-healing applications: An eco-friendly approach. *Saudi J. Biol. Sci.* **2020**, *27*, 3529–3540. [[CrossRef](#)]
19. Tran, T.N.; Doan, C.T.; Nguyen, V.B.; Nguyen, A.D.; Wang, S.L. Conversion of fishery waste to proteases by *Streptomyces speibonae* and their application in antioxidant preparation. *Fishes* **2022**, *7*, 140. [[CrossRef](#)]
20. Sharma, P.; Sharma, N. RSM approach to pre-treatment of lignocellulosic waste and a statistical methodology for optimizing bioethanol production. *Waste Manag. Bull.* **2024**, *2*, 49–66. [[CrossRef](#)]
21. Khangkhachit, W.; Suyotha, W.; Leamdum, C. Production of thermostable xylanase using *Streptomyces thermocarboxydus* ME742 and application in enzymatic conversion of xylan from oil palm empty fruit bunch to xylooligosaccharides. *Biocatal. Agric. Biotechnol.* **2021**, *37*, 102180. [[CrossRef](#)]
22. Wu, H.; Cheng, X.; Zhu, Y.; Zeng, W.; Chen, G.; Liang, Z. Purification and characterization of a cellulase-free, thermostable endo-xylanase from *Streptomyces griseorubens* LH-3 and its use in biobleaching on eucalyptus kraft pulp. *J. Biosci. Bioeng.* **2018**, *125*, 46–51. [[CrossRef](#)] [[PubMed](#)]
23. Sinjaroonsak, S.; Chaiyaso, T.; H-Kittikun, A. Optimization of cellulase and xylanase productions by *Streptomyces thermocrophilus* TC13W using low cost pretreated oil palm empty fruit bunch. *Waste Biomass Valori.* **2019**, *11*, 3925–3936. [[CrossRef](#)]
24. Blasi, A.; Verardi, A.; Lopresto, C.G.; Siciliano, S.; Sangiorgio, P. Lignocellulosic agricultural waste valorization to obtain valuable products: An overview. *Recycling* **2023**, *8*, 61. [[CrossRef](#)]

25. Ketsakhon, P.; Thammasittirong, A.; Thammasittirong, S.N. Adding value to rice straw waste for high-level xylanase production using a new isolate of *Bacillus altitudinis* RS3025. *Folia Microbiol.* **2023**, *68*, 87–99. [[CrossRef](#)] [[PubMed](#)]
26. Gautério, G.V.; da Silva, L.G.G.; Hübner, T.; da Rosa Ribeiro, T.; Kalil, S.J. Maximization of xylanase production by *Aureobasidium pullulans* using a by-product of rice grain milling as xylan source. *Biocatal. Agric. Biotechnol.* **2020**, *23*, 101511. [[CrossRef](#)]
27. Tanwar, E.; Nagar, S.; Kumari, K.; Mallesh, G.; Goyal, S. Enrichment of papaya juice using covalently immobilized xylanase from *Bacillus pumilus* SV-85S. *Biomass Conv. Bioref.* **2022**, *17*, 1–17. [[CrossRef](#)]
28. Alokika; Singh, B. Enhanced production of bacterial xylanase and its utility in saccharification of sugarcane bagasse. *Bioprocess. Biosyst. Eng.* **2020**, *43*, 1081–1091. [[CrossRef](#)] [[PubMed](#)]
29. Jnawali, P.; Kumar, V.; Tanwar, B.; Hirdyani, H.; Gupta, P. Enzymatic production of xylooligosaccharides from brown coconut husk treated with sodium hydroxide. *Waste Biomass Valoriz.* **2017**, *9*, 1757–1766. [[CrossRef](#)]
30. Zang, H.; Du, X.; Wang, J.; Cheng, Y.; Wang, Y.; Sun, S.; Zhao, X.; Li, D.; Zhang, H.; Li, C. Insight into cold-active xylanase production and xylan degradation pathways in psychrotrophic *Acinetobacter* sp. HC4 from the cold region of China. *Cellulose* **2020**, *27*, 7575–7589. [[CrossRef](#)]
31. Ire, F.S.; Chima, I.J.; Ezebuoro, V. Enhanced xylanase production from UV-mutated *Aspergillus niger* grown on corn cob and sawdust. *Biocatal. Agric. Biotechnol.* **2021**, *31*, 101869. [[CrossRef](#)]
32. Tran, T.N.; Doan, C.T.; Wang, S.L. Conversion of wheat bran to xylanases and dye adsorbent by *Streptomyces thermocarboxydis*. *Polymers* **2021**, *13*, 287. [[CrossRef](#)] [[PubMed](#)]
33. Iram, A.; Cekmecelioglu, D.; Demirci, A. Optimization of the fermentation parameters to maximize the production of cellulases and xylanases using DDGS as the main feedstock in stirred tank bioreactors. *Biocatal. Agric. Biotechnol.* **2022**, *45*, 102514.
34. Prabha, B.; Ramesh, D.; Sriramajayam, S.; Uma, D. Optimization of pyrolysis process parameters for fuel oil production from the thermal recycling of waste polypropylene grocery bags using the Box–Behnken design. *Recycling* **2024**, *9*, 15. [[CrossRef](#)]
35. Lenth, R.V. Response-Surface Methods in R, Using rsm. *J. Stat. Softw.* **2009**, *30*, 7–15.
36. Sanjivkumar, M.; Silambarasan, T.; Balagurunathan, R.; Immanuel, G. Biosynthesis, molecular modeling and statistical optimization of xylanase from a mangrove associated actinobacterium *Streptomyces variabilis* (MAB3) using Box–Behnken design with its bioconversion efficacy. *Int. J. Biol. Macromol.* **2018**, *118*, 195–208. [[CrossRef](#)] [[PubMed](#)]
37. Medouni-Haroune, L.; Medouni-Adar, S.; Houfani, A.A.; Bouiche, C.; Azzouz, Z.; Roussos, S.; Desseaux, V.; Madani, K.; Kecha, M. Statistical optimization and partial characterization of xylanases produced by *Streptomyces* sp. S1M3I using olive pomace as a fermentation substrate. *Appl. Biochem. Biotechnol.* **2024**, *196*, 2012–2013. [[CrossRef](#)] [[PubMed](#)]
38. Kim, D.Y.; Han, M.K.; Oh, H.W.; Park, D.S.; Kim, S.J.; Lee, S.G.; Shin, D.H.; Son, K.H.; Bae, K.S.; Park, H.Y. Catalytic properties of a GH10 endo- β -1, 4- xylanase from *Streptomyces thermocarboxydis* HY-15 isolated from the gut of *Eisenia fetida*. *J. Mol. Catal. B Enzym.* **2010**, *62*, 32–39. [[CrossRef](#)]
39. Chi, W.J.; Lim, J.H.; Park, D.Y.; Park, J.S.; Hong, S.K. Production and characterization of a thermostable endo-type β -xylanase produced by a newly-isolated *Streptomyces thermocarboxydis* subspecies MW8 strain from Jeju Island. *Process Biochem.* **2013**, *48*, 1736–1743. [[CrossRef](#)]
40. Boonchuay, P.; Takenaka, S.; Kuntiya, A.; Techapun, C.; Leksawasdi, N.; Seesuriyachan, P.; Chaiyaso, T. Purification, characterization, and molecular cloning of the xylanase from *Streptomyces thermovulgaris* TISTR1948 and its application to xylooligosaccharide production. *J. Mol. Catal. B Enzym.* **2016**, *129*, 61–68. [[CrossRef](#)]
41. He, J.; Su, L.; Sun, X.; Fu, J.; Chen, J.; Wu, J. A novel xylanase from *Streptomyces* sp. FA1: Purification, characterization, identification, and heterologous expression. *Biotechnol. Bioproc. E* **2014**, *19*, 8–17. [[CrossRef](#)]
42. Yan, Q.; Hao, S.; Jiang, Z.; Zhai, Q.; Chen, W. Properties of a xylanase from *Streptomyces matensis* being suitable for xylooligosaccharides production. *J. Mol. Catal. B Enzym.* **2009**, *58*, 72–77. [[CrossRef](#)]
43. Ninawe, S.; Kapoor, M.; Kuhad, R.C. Purification and characterization of extracellular xylanase from *Streptomyces cyaneus* SN32. *Bioresour. Technol.* **2007**, *99*, 1252–1258. [[CrossRef](#)] [[PubMed](#)]
44. Qiu, Z.; Shi, P.; Luo, H.; Bai, Y.; Yuan, T.; Yang, P.; Liu, S.; Yao, B. A xylanase with broad pH and temperature adaptability from *Streptomyces megasporus* DSM 41476, and its potential application in brewing industry. *Enzyme Microb. Technol.* **2010**, *46*, 506–512. [[CrossRef](#)] [[PubMed](#)]
45. Zhu, W.; Qin, L.; Xu, Y.; Lu, H.; Wu, Q.; Li, W.; Zhang, C.; Li, X. Three molecular modification strategies to improve the thermostability of xylanase XynA from *Streptomyces rameus* L2001. *Foods* **2023**, *12*, 879. [[CrossRef](#)] [[PubMed](#)]
46. Li, X.; Li, E.; Zhu, Y.; Teng, C.; Sun, B.; Song, H.; Yang, R. A typical endoxylanase from *Streptomyces rameus* L2001 and its unique characteristics in xylooligosaccharide production. *Carbohydr. Res.* **2012**, *359*, 30–36. [[CrossRef](#)] [[PubMed](#)]
47. Yang, R.; Li, J.; Teng, C.; Li, X. Cloning, overexpression and characterization of a xylanase gene from a novel *Streptomyces rameus* L2001 in *Pichia pastoris*. *J. Mol. Catal. B-Enzym.* **2016**, *131*, 85–93. [[CrossRef](#)]
48. Mander, P.; Choi, Y.H.; Pradeep, G.C.; Choi, Y.S.; Hong, J.H.; Cho, S.S.; Yoo, J.C. Biochemical characterization of xylanase produced from *Streptomyces* sp. CS624 using an agro residue substrate. *Process Biochem.* **2014**, *49*, 451–456. [[CrossRef](#)]
49. Manicardi, T.; Baioni e Silva, G.; Longati, A.A.; Paiva, T.D.; Souza, J.P.M.; Pádua, T.F.; Furlan, F.F.; Giordano, R.L.C.; Giordano, R.C.; Milessi, T.S. xylooligosaccharides: A bibliometric analysis and current advances of this bioactive food chemical as a potential product in biorefineries' portfolios. *Foods* **2023**, *12*, 3007. [[CrossRef](#)]

50. Kim, D.; Yu, J.; Hong, K.; Jung, C.; Kim, H.; Kim, J.; Myung, S. Green production of low-molecular-weight xylooligosaccharides from oil palm empty fruit bunch via integrated enzymatic polymerization and membrane separation for purification. *Sep. Purif. Technol.* **2022**, *293*, 121084. [[CrossRef](#)]
51. Miller, G.L. Use of dinitrosalicylic acid reagent for determination of reducing sugar. *Anal. Chem.* **1959**, *31*, 426–428. [[CrossRef](#)]
52. Lowry, O.H.; Rosebrough, N.J.; Farr, A.L.; Randall, R.J. Protein measurement with the Folin phenol reagent. *J. Biol. Chem.* **1951**, *193*, 265–275. [[CrossRef](#)] [[PubMed](#)]
53. Doan, C.T.; Tran, T.N.; Nguyen, V.B.; Nguyen, A.D.; Wang, S.L. Utilization of seafood processing by-products for production of proteases by *Paenibacillus* sp. TKU052 and their application in biopeptides' preparation. *Mar. Drugs* **2020**, *18*, 574. [[CrossRef](#)] [[PubMed](#)]
54. Doan, C.T.; Tran, T.N.; Tran, T.P.H.; Nguyen, T.T.; Nguyen, H.K.; Tran, T.K.T.; Vu, B.T.; Trinh, T.H.T.; Nguyen, A.D.; Wang, S.L. Chitosanase production from the liquid fermentation of squid pens waste by *Paenibacillus elgii*. *Polymers* **2023**, *15*, 3724. [[CrossRef](#)]

Disclaimer/Publisher's Note: The statements, opinions and data contained in all publications are solely those of the individual author(s) and contributor(s) and not of MDPI and/or the editor(s). MDPI and/or the editor(s) disclaim responsibility for any injury to people or property resulting from any ideas, methods, instructions or products referred to in the content.